Research Article | Vol. 9, No. 5 / 1 May 2019 / Optical Materials Express 2368

Optical Materials EXPRESS

Radiation trapping in selected Er^{3+} doped chalcogenide glasses and the extraction of the nonradiative lifetime

CYRIL KOUGHIA,[1,*] CHRIS CRAIG,[2] DANIEL W. HEWAK,[2] AND SAFA KASAP[1]

[1]Department of Electrical and Computer Engineering, University of Saskatchewan, Saskatoon, Canada
[2]Optoelectronics Research Centre, University of Southampton, Southampton, SO17 1BJ, UK
*cyril.koughia@usask.ca

Abstract: Radiation trapping (RT) is a phenomenon wherein photons are emitted, absorbed and re-emitted many times before they leave the volume of the material. Trivalent Er^{3+} ions are particularly prone to RT because there is a whole set of strongly overlapping emission and absorption bands including $^4I_{13/2}$–$^4I_{15/2}$ and $^4I_{11/2}$–$^4I_{15/2}$ bands. The effect of RT on the PL decay time was investigated experimentally in this work in a variety of Er^{3+}-doped GeGaS, GeGaSe, GaLaS(O) glasses. Sample geometry (powders, plates, disks, cylinders) and size were varied and the samples were also immersed in glycol, a liquid with high refractive index. PL decay times were measured and compared with the Judd-Ofelt results. A simple model of RT was developed and applied to the above mentioned bands. By comparing model conclusions with experimental data for different sample sizes, we were able to separate the direct relaxation of the $^4I_{11/2}$ state to ground $^4I_{15/2}$ state and relaxation via the intermediate $^4I_{13/2}$ state; and hence obtain an approximate nonradiative lifetime.

1. Introduction

Radiation trapping (RT) is a phenomenon wherein photons are emitted, absorbed and re-emitted many times before they leave the volume of the material. RT has been observed and reported in a variety of materials where there is a strong overlap of the emission and absorption bands. Historically, its discovery dates back to the mid-1920s [1,2]. Indeed, Lucy Hayner's paper in 1925 included a term "radiation imprisonment" to describe the delay involved in the passage of luminescence radiation through an Hg vapor [1]. Over the last two decades it has been widely observed in materials doped with multivalent rare earth ions [3–13]. Among various rare earths ions, the trivalent Er^{3+} offers a unique opportunity for RT because there is a whole set of perfectly overlapping emission and absorption bands [14]. Usually, RT is regarded a 'nuisance' that leads to the distortion of PL spectra and radiative lifetimes [3,11]. Researchers try to eliminate RT by experimenting on fine powders [7,11] or by using excitation and detection through spatially separated pinholes [15–17] or by using a confocal setup [18].

In the present work, we use RT as a means of separating the direct relaxation of $^4I_{11/2}$ state to ground $^4I_{15/2}$ state and relaxation via intermediate $^4I_{13/2}$ state. Based on our previous findings [19], we build a simple model of RT. We apply this model to $^4I_{13/2}$–$^4I_{15/2}$ and $^4I_{11/2}$–$^4I_{15/2}$ bands of Er^{3+} embedded in several chalcogenide glasses with different compositions and offer a way to separate direct radiative transition and non-radiative relaxation of the $^4I_{11/2}$ state.

#356716 https://doi.org/10.1364/OME.9.002368
Journal © 2019 Received 2 Jan 2019; revised 29 Mar 2019; accepted 30 Mar 2019; published 29 Apr 2019

Optical Materials EXPRESS

2. Experimental procedure

Er^{3+} doped glasses were prepared by melt quenching of raw materials mixed in the proportions shown in Table 1. The lanthanum sulphide-oxide glasses (rows 1 and 2 in Table 1) were prepared at the University of Southampton. The detailed description of their preparation technique may be found elsewhere [19]. The germanium gallium sulphide (3) and germanium gallium selenide (4) glasses were synthesized at the University of Saskatchewan. The synthesis details have been described in Refs. [20,21].

Table 1. Glass compositions; E_g - optical gap; $\tau_{10}(0)$ and $\tau_{20}(0)$ PL decay times in fine powders for $^4I_{13/2}$–$^4I_{15/2}$ and $^4I_{11/2}$–$^4I_{15/2}$ bands, respectively; a - slope of the straight lines in Fig. 3; τ_{20} and τ_{21} relaxation times of $^4I_{11/2}$–$^4I_{15/2}$ and $^4I_{11/2}$–$^4I_{13/2}$, respectively (deduced in the present paper). Optical gap (E_g) is accepted to be equal to the photon energy at which absorption coefficient is equal to 10^3 cm^{-1}.

	Glass compositions	E_g, eV	$\tau_{10}(0)$, ms	$\tau_{20}(0)$, ms	a	τ_{20} , ms	τ_{21} , ms
1	73 Ga_2S_3 + 27 La_2O_3 + 0.5 Er_2O_3	3.05	3.35	0.89	0.22	3.98	1.15
2	66 Ga_2S_3 + 32 La_2S_3 + 3 La_2O_3 + 0.5 Er_2O_3	2.79	2.73	1.40	0.53	2.62	2.98
3	90 GeS_2 + 10 Ga_2S_3 + 0.5 Er_2S_3	3.00	2.71	1.58	0.40	3.96	2.63
4	90 $GeSe_2$ + 10 Ga_2Se_3 + 0.5 Er_2S_3	2.31	1.91	0.94	0.59	1.60	2.29

The effects of photon trapping depend on the sample geometry. Following a geometrically wise approach, we have used three types of samples (as an illustration, see inset of Fig. 2).

(1) *Fine powders* with an average particle diameter around 30 μm were prepared by crushing bulk materials and passing them through a sequence of sieves with appropriate meshes. The powders were collected on a sticky scotch tape. A control experiment confirmed the absence of a PL response from the virgin scotch tape.

(2) The optical *plates* were cut off from a glass rod (diameter around 2 mm) and had typical thickness around 1 mm. They were polished on both sides for optical transmittance and PL measurements.

(3) *Cylinders* were cut off from the same glass rod and polished on both sides. The length of cylinders varied from 10 to 44 mm. As a result of polishing, the cylinders had all shiny surfaces favoring an effective "imprisonment" of light due to internal reflection. For some of the experiments, the samples were submerged in glycol, a liquid with high refractive index. More details on sample preparation and experiments involving glycol submersion may be found in Ref. [19].

PL corresponding to $^4I_{13/2}$–$^4I_{15/2}$ and $^4I_{11/2}$–$^4I_{15/2}$ transitions in Er^{3+} ions was dispersed by Cornerstone monochromator and detected using Peltier cooled InGaAs detector. The excitation corresponding to the $^4I_{15/2}$–$^4I_{9/2}$ transition in Er^{3+} ions was performed by laser diode operating at 808 nm. A ORIEL mechanical chopper was used for transient PL measurements and the signal from the InGaAs detector built-in-amplifier was directly coupled to PicoScope oscilloscope for registration and further analysis.

It should be mentioned that GaLaS(O) glasses used in this work have negligible OH^- content as reported previously and confirmed by the absorption spectra around 3 μm [22]. In the case of GeGaS and GeGaSe glasses, the addition of Ga leads to a large increase in the solubility of Er^{3+} in this glass system, especially if stoichiometric compositions of constituent compounds are alloyed as in this work [21]. Further, the Er^{3+} concentration used in this work is much less than that needed for concentration quenching [7] and the results and conclusions are not affected by the latter phenomenon.

Optical Materials EXPRESS

3. Experimental results

Figure 1 compares the PL decays from the steady-state after cessation of excitation at 808 nm in samples of Er^{3+} doped gallium lanthanum sulphide-oxide glasses with two different compositions marked as samples 1 and 2 in Table 1. The measurements were performed for two different emission bands $^4I_{13/2}$–$^4I_{15/2}$ and $^4I_{11/2}$–$^4I_{15/2}$. The fastest PL decays were observed in powdered materials with particle size $L \approx 30\,\mu m$. As the geometrical size of samples becomes bigger, the PL decays become slower. This effect was observed in all investigated glasses in this work and for both emission bands.

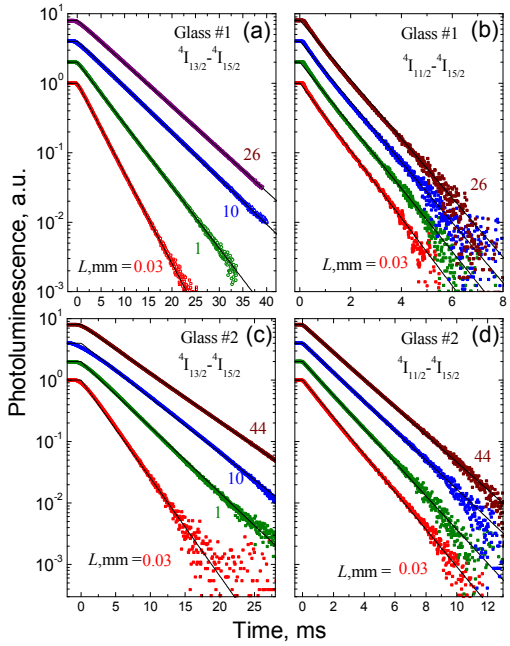

Fig. 1. The influence of geometrical size on PL decays from steady-state after switching-off the excitation in two samples with compositions shown in Table 1 and for two emission bands. The meaning of sample size (L) is explained in the caption of Fig. 2. Solid lines are the best single exponential fits to experimental data. All experiments are performed in air. Excitation is by a laser diode at 808 nm.

Figure 2 depicts the dependence of PL decay times on the geometrical size of samples. This figure illustrates that the rate of increase depends on the glass composition and the emission band. Thus, changes of PL decay time are less pronounced for glass 1 than glass 2 in particular for $^4I_{11/2}$–$^4I_{15/2}$ emission band. Figure 2 shows also the acceleration of PL decay (reduction of decay time) when the sample is submersed in glycol.

Here and after we will refer to $^4I_{15/2}$ manifold as the ground or 0^{th} level, to $^4I_{13/2}$ as 1^{st} level and to $^4I_{11/2}$ as 2^{nd} level. Accordingly, the measured PL decay times for $^4I_{13/2}$–$^4I_{15/2}$ transitions in fine powders and bulk materials will be referred to as $\tau_1(0)$ and $\tau_1(L)$, respectively. Similar notations $\tau_2(0)$ and $\tau_2(L)$ will be used for PL decay times for $^4I_{11/2}$–$^4I_{15/2}$ transitions in fine powders and bulk materials, respectively. Figure 3 compares the ratios of PL decay times for $^4I_{11/2}$–$^4I_{15/2}$ and $^4I_{11/2}$–$^4I_{15/2}$ emission bands for different glasses. It shows linear dependence in a form

$$\frac{\tau_2(0)}{\tau_2(L)} = a\frac{\tau_1(0)}{\tau_1(L)} + (1-a) \tag{1}$$

Optical Materials EXPRESS

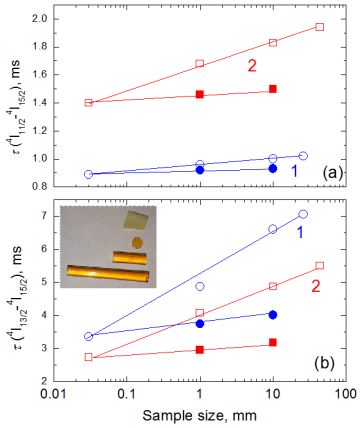

Fig. 2. The PL decay times vs. geometrical size of samples for $^4I_{11/2}$–$^4I_{15/2}$ (upper pane (a)) and $^4I_{13/2}$–$^4I_{15/2}$ (lower pane (b)) emission bands. Numbers 1 and 2 stand for two different glass compositions as shown in Table 1. Open symbols are results collected in air. Full symbols show the results for samples submersed in glycol. Powders in air and in glycol give coinciding results. The inset to figure (b) illustrates the geometry of samples (glass #1) used in the present research. The samples of fine powders with particle size ($L \approx$ 0.03 mm) were collected on scotch tape. Round optical plates had a diameter close to 2 mm and thickness ($L \approx 1$ mm (shown in the inset)). Cylinders with both polished ends had a diameter close to 2 mm and varying heights ($L = 10$, 26 and 44 mm. Cylinders with $L = 10$ and 26 mm are shown in the inset). Solid lines are guides to the eye.

where a is a slope with values listed in Table 1. The meaning of the graphs and the importance of linearity are explained and discussed in detail in the next section.

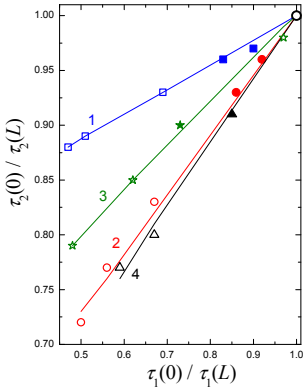

Fig. 3. Ratio of PL decay times $\tau_2(L)/\tau_2(0)$ versus ratio $\tau_1(L)/\tau_1(0)$. Here $\tau_2(L)$ is the PL decay time for Er^{3+} $^4I_{11/2}$–$^4I_{15/2}$ emission band in bulk samples; $\tau_2(0)$ is the PL decay time for the same band in fine powders; $\tau_1(L)$ is the PL decay time for Er^{3+} $^4I_{13/2}$–$^4I_{15/2}$ emission band in bulk samples and $\tau_1(0)$ is the PL decay time for the same band in fine powders. Numbers from 1 to 4 correspond to different glass compositions as listed in Table 1. Open symbols are results collected in air. Full symbols are for samples submersed in glycol. Solid lines are least square fits to experimental data using Eq. (1) with slopes a listed in Table 1.

Optical Materials EXPRESS

4. Model and discussion

In this section, a simplistic model of radiation trapping is developed. Let N_i be the *total number* of excited ions in the *whole* sample. Suppose excited ions may relax through two independent processes with characteristic times τ_1 and τ_2. In this case, the decay of N_i after switching-off the excitation may be described by a simple rate equation

$$\frac{dN_i}{dt} = -\frac{N_i}{\tau_1} - \frac{N_i}{\tau_2} \tag{2}$$

The solution of Eq. (2) will obviously be a single exponential decay with a characteristic time

$$\tau(0) = \frac{\tau_1\tau_2}{\tau_1 + \tau_2} \tag{3}$$

For the future let us assume that the first process (with characteristic time τ_1) is a radiative transition. Experimentally, $\tau(0)$ may be observed in fine powders where the influence of RT has been proven to be negligible, as, for example, in Refs. [7,11]. However in the presence of RT some modifications of Eq. (2) are required. First of all, we note that the radiative transition becomes "less efficient" because part of emitted PL photons is reabsorbed by Er^{3+} ions. Therefore, Eq. (2) should be corrected as

$$\frac{dN_i}{dt} = -\frac{N_i}{\tau_1}p_{esc}(L) - \frac{N_i}{\tau_2} \tag{4}$$

here $p_{esc}(L)$ is the probability of photon to escape the sample with the size L without being reabsorbed. Obviously, the parameter p_{esc} depends on the sample size. Thus, in fine powders, $p_{esc}(L)\rightarrow 1$ due to the small size of powder particles and the inefficiency of reabsorption. On the other hand, in large samples $p_{esc}(L)\rightarrow 0$, meaning that nearly all photons are being reabsorbed within a huge volume of the sample. The solution of Eq. (4) gives again a single exponential decay but with a different characteristic time

$$\tau(L) = \frac{\tau_1\tau_2}{\tau_1 + \tau_2 p_{esc}(L)} \tag{5}$$

which is observed in bulk samples with *effective geometrical size L* as PL decay time. Dividing Eq. (3) by (5) we find the ratio of two characteristic PL decay times in powdered and bulk materials as

$$\frac{\tau(0)}{\tau(L)} = \frac{\tau_1}{\tau_1 + \tau_2} + \frac{\tau_2}{\tau_1 + \tau_2}p_{esc}(L) \tag{6}$$

Equation (6) is a general relation that can be applied to some particular cases. Let us start with the $^4I_{13/2}$–$^4I_{15/2}$ relaxation of Er^{3+} ions. Usually, the relaxation from $^4I_{13/2}$ level (it is referred to as level 1 in this paper) to ground level $^4I_{15/2}$ (level 0) occurs by radiative emission which is known to be the dominant relaxation process in many glasses [7,23]. In other words, there is only one relaxation mechanism and hence Eq. (6) may be reduced to

$$\frac{\tau_1(0)}{\tau_1(L)} = p_{esc}^{(1)}(L) \tag{7}$$

here the index (1) shows that Eq. (7) refers to the first emission/absorption band, i.e. $^4I_{13/2} - {}^4I_{15/2}$.

Er^{3+} in second exited state $^4I_{11/2}$ may relax either directly to the $^4I_{15/2}$ ground state or through an intermediate excited $^4I_{13/2}$ state. The first $^4I_{11/2}$–$^4I_{15/2}$ relaxation is purely radiative and may be strongly affected by RT due to the presence of the matching $^4I_{15/2}$–$^4I_{11/2}$ absorption band. The presence of RT is supported by Fig. 1 and reported earlier for some other glasses [3–7,14]. Let us assume that $^4I_{11/2}$–$^4I_{15/2}$ radiative lifetime is τ_{20}.

Optical Materials EXPRESS

The relaxation from $^4I_{11/2}$ to $^4I_{13/2}$ state may be radiative or non-radiative. Obviously, for non-radiative relaxation there is no RT. However, for $^4I_{11/2}$–$^4I_{13/2}$ radiative relaxation the RT influence is also negligible because detectable $^4I_{13/2}$–$^4I_{11/2}$ excitation stimulated absorption appears only at very high pumping levels far exceeding those used in present paper. Assuming that the radiative lifetime is $\tau_{21}^{(R)}$ and non-radiative relaxation time is τ_{21}^{NR})we get an effective time of relaxation from $^4I_{11/2}$ to $^4I_{13/2}$ as $\tau_{21} = (1/\tau_{21}^{(R)} + 1/\tau_{21}^{(NR)})^{-1}$ and in the case of relaxation of $^4I_{11/2}$ level, Eq. (6) may be presented as

$$\frac{\tau_2(0)}{\tau_2(L)} = \frac{\tau_{20}}{\tau_{20}+\tau_{21}} + \frac{\tau_{21}}{\tau_{20}+\tau_{21}} p_{esc}^{(2)}(L) \tag{8}$$

By combining experimental results presented by Eq. (1) with Eqs. (7) and (8), it is easy to derive the relation between $p_{esc}^{(1)}(L)$and $p_{esc}^{(2)}(L)$as

$$\frac{\tau_{20}}{\tau_{20}+\tau_{21}} + \frac{\tau_{21}}{\tau_{20}+\tau_{21}} p_{esc}^{(2)}(L) = (1-a) + a p_{esc}^{(1)}(L) \tag{9}$$

In very big samples ($L \to \infty$), as we already mentioned earlier, the escape becomes improbable, i.e. $p_{esc} \to 0$ for both bands giving us a simple relation between τ_{20} , τ_{21} and the experimental value of a

$$\frac{\tau_{20}}{\tau_{20}+\tau_{21}} = (1-a) \qquad \text{or} \qquad a = \frac{\tau_{21}}{\tau_{21}+\tau_{20}} \tag{10}$$

Equation (10) is the final result of our simple model and it shows that the slope of the linear dependence (a) in Eq. (1) may be used to evaluate τ_{20} and τ_{21} as

$$\tau_{20} = \frac{\tau_2(0)}{a} \qquad \text{and} \qquad \tau_{21} = \frac{\tau_2(0)}{1-a} \tag{11}$$

The results of these calculations for four different glasses doped with Er^{3+} ions are summarized and presented in Table 1. The validity of these conclusions is presented in Table 2 which compares the predicted values of τ_{20} with calculations using Judd-Ofelt model. In overall,

Table 2. Glass compositions; Judd-Ofelt parameters (Ω_2, Ω_4 and Ω_6) ; β - branching ratio for level $^4I_{11/2}$; R_{10}^{ed}- electric dipole $^4I_{13/2}$–$^4I_{15/2}$ transition rate; R_{10}^{md}- magnetic dipole $^4I_{13/2}$ –$^4I_{15/2}$ transition rate; τ_{10}^{JO}- calculated $^4I_{13/2}$ –$^4I_{15/2}$ transition radiative lifetime; R_{20}^{ed}- electric dipole $^4I_{11/2}$ –$^4I_{15/2}$ transition rate; τ_{20}^{JO}- calculated $^4I_{11/2}$ –$^4I_{15/2}$ transition radiative lifetime. The values of $\tau_{10}(0)$ and τ_{20} are reproduced from Table 1 to facilitate comparison with τ_{10}^{JO} and τ_{20}^{JO}, respectively. The values for Judd-Ofelt parameters for glasses 3 and 4 were published previously in [24] and [7], respectively.

	Glass compositions	Ω_2 (10^{-20}cm^2)	Ω_4 (10^{-20}cm^2)	Ω_6 (10^{-20}cm^2)	β (%)	R_{10}^{ed} (s^{-1})	R_{10}^{md} (s^{-1})	τ_{10}^{JO} (ms)	$\tau_{10}(0)$ (ms)	R_{20}^{ed} (s^{-1})	τ_{20}^{JO} (ms)	τ_{20} (ms)
1	73 Ga_2S_3 + 27 La_2O_3 + 0.5 Er_2O_3	6.78	1.17	0.49	14	186	112	3.36	3.35	267	3.75	3.98
2	66 Ga_2S_3 + 32 La_2S_3 + 3 La_2O_3 + 0.5 Er_2O_3	6.22	1.92	0.49	14	236	127	2.75	2.73	402	2.49	2.62
3	90 GeS_2 + 10 Ga_2S_3 + 0.5 Er_2S_3	11	2.9	1.6	11	314	70	2.60	2.71	349	2.87	3.96
4	90 $GeSe_2$ + 10 Ga_2Se_3 + 0.5 Er_2S_3	8.6	2.1	1.1	12	417	117	1.87	1.91	699	1.43	1.6

Optical Materials EXPRESS

Table 2 shows quite good agreement of $^4I_{13/2}$–$^4I_{15/2}$ radiative recombination times τ_{10}^{JO} with experimental values of PL decay times in fine powders $\tau_{10}(0)$, confirming the applicability of the JO model to our case. Table 2 also shows a reasonable agreement of values of $^4I_{13/2}$–$^4I_{15/2}$ radiative recombination times τ_{20}^{JO} and τ_{20} which are calculated in the present paper.

5. Conclusions

We investigated radiation trapping in four different classes of Er^{3+} doped chalcogenide glasses. Radiation trapping appears in materials in which there is a strong overlap of emission and absorption spectra. From this point of view, Er^{3+} ions are ideal the manifestation of radiation trapping as they possess many overlapping absorption and emission bands including $^4I_{13/2}$–$^4I_{15/2}$ and $^4I_{11/2}$–$^4I_{15/2}$. We have developed a simple model for radiation trapping that incorporates the sample size effect into the observed PL decay time, and applied this model to the above mentioned bands in Er^{3+} ions in four different chalcogenide glass hosts. By comparing model conclusions with experimental data for different sample sizes, we were able to separate the direct relaxation of $^4I_{11/2}$ state to ground $^4I_{15/2}$ state and relaxation via the intermediate $^4I_{13/2}$ state. This procedure was shown to be effective for four different glasses with very different compositions.

Funding

Natural Sciences and Engineering Research Council of Canada (NSERC) (Discovery Grants); Engineering and Physical Sciences Research Council (EPSRC) (EP/M015130/1).

Acknowledgments

Saskatchewan acknowledges NSERC Discovery Grants for financial support. Southampton acknowledged the support of the Engineering and Physical Sciences Research Council, United Kingdom, through a grant EP/M015130/1, Manufacturing and Application of Next Generation Chalcogenides.

References

1. L. J. Hayner, "The persistence of the radiation excited in mercury vapor," Phys. Rev. **26**(3), 364–375 (1925).
2. E. A. Milne, "The diffusion of imprisoned radiation through a gas," J. London Math. Soc. **s1-1**(1), 40–51 (1926).
3. W. Chung, A. Jha, S. Shen, and P. Joshi, "The effect of Er^{3+}-ion concentration on the Er^{3+}:$^4I_{13/2}$→$^4I_{15/2}$ transition in tellurite glasses," Philos. Mag. **84**(12), 1197–1207 (2004).
4. F. Auzel, F. Bonfigli, S. Gagliari, and G. Baldacchini, "The interplay of self-trapping and self-quenching for resonant transitions in solids; Role of a cavity," J. Lumin. **94-95**(95), 293–297 (2001).
5. F. Auzel, G. Baldacchini, L. Laversenne, and G. Boulon, "Radiation trapping and self-quenching analysis in Yb^{3+}, Er^{3+}, and Ho^{3+} doped Y_2O_3," Opt. Mater. **24**(1-2), 103–109 (2003).
6. B. Richards, S. Shen, A. Jha, Y. Tsang, and D. Binks, "Infrared emission and energy transfer in Tm^{3+}, Tm^{3+}-Ho^{3+} and Tm^{3+}-Yb^{3+}-doped tellurite fibre," Opt. Express **15**(11), 6546–6551 (2007).
7. C. Koughia and S. O. Kasap, "Excitation diffusion in GeGaSe and GeGaS glasses heavily doped with Er^{3+}," Opt. Express **16**(11), 7709–7714 (2008).
8. C. Koughia, C. Craig, D. W. Hewak, and S. Kasap, "Tailoring the $^4I_{9/2}$→$^4I_{13/2}$ emission in Er^{3+} ions in different hosts media," Opt. Mater. **41**, 116–121 (2015).
9. J. A. Muñoz, B. Herreros, G. Lifante, and F. Cussó, "Concentration dependence of the 1.5 mm emission lifetime of Er^{3+} in $LiNbO_3$ by radiation trapping," Phys. Stat. Sol.(a) **168**(2), 525–530 (1998).
10. D. S. Sumida and T. Y. Fan, "Effects of radiation trapping on fluorescence lifetime and emission cross section measurements in solid-state laser media," Opt. Lett. **19**(17), 1343–1345 (1994).
11. M. Mattarelli, M. Montagna, L. Zampedri, A. Chiasera, M. Ferrari, G. C. Righini, L. M. Fortes, M. C. Gonçalves, L. F. Santos, and R. M. Almeida, "Self-absorption and radiation trapping in Er^{3+}-doped TeO_2-based glasses," Europhys. Lett. **71**(3), 394–399 (2005).
12. V. G. Babajanyan, R. B. Kostanyan, and P. H. Muzhikyan, "Spectral and kinetic peculiarities of the radiation trapping effect in doped materials," Opt. Mater. **45**, 215–218 (2015).
13. W. C. Wang, W. J. Zhang, L. X. Li, Y. Liu, D. D. Chen, Q. Qian, and Q. Y. Zhang, "Spectroscopic and structural characterization of barium tellurite glass fibers for mid-infrared ultra-broad tunable fiber lasers," Opt. Mater. Express **6**(6), 2095–2107 (2016).

Optical Materials EXPRESS

14. S. Kasap and C. Koughia, "The influence of radiation trapping on spectra and measured lifetimes of $^4F_{9/2}$ -$^4I_{15/2}$, $^4I_{9/2}$ –$^4I_{15/2}$, $^4I_{11/2}$–$^4I_{15/2}$ and $^4I_{13/2}$–$^4I_{15/2}$ emission bands in GeGaS glasses doped with erbium," *Int. Conf. Transparent Opt. Networks.* 2016–August (2016) 13–17. doi:10.1109/ICTON.2016.7550252.
15. H. Kühn, S. T. Fredrich-Thornton, C. Kränkel, R. Peters, and K. Petermann, "Model for the calculation of radiation trapping and description of the pinhole method," Opt. Lett. **32**(13), 1908–1910 (2007).
16. G. Toci, "Lifetime measurements with the pinhole method in presence of radiation trapping," Appl. Phys. B: Lasers Opt. **106**(1), 63–71 (2012).
17. G. Toci, D. Alderighi, A. Pirri, and M. Vannini, "Lifetime measurements with the pinhole method in presence of radiation trapping: II - Application to Yb^{3+} doped ceramics and crystals," Appl. Phys. B: Lasers Opt. **106**(1), 73–79 (2012).
18. Y.-S. Yong, S. Aravazhi, S. A. Vázquez- Córdova, J. J. Carvajal, F. Díaz, J. L. Herek, S. M. García-Blanco, and M. Pollnau, "Direct confocal lifetime measurements on rare-earth-doped media exhibiting radiation trapping," Opt. Mater. Express **7**(2), 527–532 (2017).
19. C. Koughia, C. Craig, D.W. Hewak, and S. Kasap, "Further studies of radiation trapping in Er^{3+} doped chalcogenide glasses," Opt. Mater. **87**, 157–163 (2019).
20. K. Koughia, M. Munzar, D. Tonchev, C. J. Haugen, R. G. Decorby, J. N. McMullin, and S. O. Kasap, "Photoluminescence in Er-doped Ge-Ga-Se glasses," J. Lumin. **112**(1-4), 92–96 (2005).
21. M. Munzar, K. Koughia, D. Tonchev, S. O. Kasap, T. Sakai, K. Maeda, T. Ikari, C. Haugen, R. Decorby, and J. N. McMullin, "Influence of Ga on the optical and thermal properties of Er^{3+} doped stoichiometric and nonstoichiometric Ge-Ga-Se glasses," Phys. Chem. Glass. **46**(2), 215–219 (2005).
22. D. W. Hewak, J. A. M. Neto, B. Samson, R. S. Brown, K. P. Jedrzejewski, and J. Wang, "Quantum-efficiency of praseodymium doped Ga:La:S glass for 1.3 micron optical fibre amplifiers," IEEE Photonics Technol. Lett. **6**(5), 609–612 (1994).
23. C. C. Ye, D. W. Hewak, M. Hempstead, B. N. Samson, and D. N. Payne, "Spectral properties of Er^{3+}-doped gallium lanthanum sulphide glass," J. Non-Cryst. Solids **208**(1-2), 56–63 (1996).
24. K. Koughia, D. Saitou, T. Aoki, M. Munzar, and S. O. Kasap, "Photoluminescence lifetime spectrum in erbium doped Ge–Ga–S glasses," J. Non-Cryst. Solids **352**(23-25), 2420–2424 (2006).